Send Orders for Reprints to reprints@benthamscience.ae

The Open Automation and Control Systems Journal, **2015,** *7,* **49-59**

Open Access

Holographic Blind Watermarking Algorithm of Three- Dimensional Mesh Model Based on QR Decomposition

Wenju Wang[1,*], Liujie Sun[1], Qin Yang[1] and Zhang Xuan[2]

[1]*University of Shanghai for Science and Technology, Shanghai 200093, China*

[2]*Shanghai Conservatory of Music, Shanghai 200031, China*

Abstract: This paper proposes a holographic blind watermarking algorithm of the three-dimensional mesh model based on QR decomposition. Firstly the three-dimensional model is pre-processed by moving the model center to the coordinate origin and doing PCA analysis. Secondly the model's geometric feature matrix is constructed by using the distance from the three-dimensional mesh model vortex to the model center in the column coordinate system. Then the watermarking information generated by the holographic encrypted technology is embedded into the normalized and blocked model's geometric feature matrix based on QR decomposition. Finally the watermark is embedded into three-dimensional mesh model via inverse QR decomposition and inverse normalization operation. The experimental results indicate that this algorithm can resist translation, rotation, scaling, vertex reordering, noise and cropping attack, which has good robustness. This method can effectively protect the three-dimensional mesh model intellectual property.

Keywords: Digital watermark, holographic encryption, QR decomposition, three-dimensional mesh mode.

1. INTRODUCTION

With increasing popularity of the network exchange and high-speed development of electronic commerce, it becomes the research focus how to effectively protect three-dimensional model in the digital publication, social content production and supervision, which spent many intelligence resource. The digital watermark of three-dimensional model is one important means to effectively protect three-dimensional model, which can prevent against infringement and piracy in information exchange. In addition, it is also very meaningful to standardize digital market and promote healthy and sustainable development of the information industry of human being [1, 2].

The three-dimensional mesh digital watermarking algorithm is divided into the space domain and transformation domain according to the working domain of the watermarking algorithm.

Transformation domain algorithm: in 1999, Praun [3] extended the spread spectrum technology of 2D digital watermark scheme into the digital watermark algorithm of the three-dimensional model. Although this method is robust, it has some weaknesses. For example, this method requires many calculations, is fully independent of the common mesh handling and editing algorithm, and will perform multi-resolution decomposition for the model. In 2001, Ohbuchi obtained the Laplace operator based on the mesh topology and realized three-dimensional mesh model watermarking algorithm by analyzing the mesh's pseudo-spectrum [4], but the embedded data is limited. In 1998, Kai wang performed wavelet decomposition for the three-dimensional mesh model and embedded the robust watermark, vulnerable watermark and high-capacity watermark into the proper wavelet resolution. This is a blind watermarking algorithm [5], but this algorithm is not very robust. In 2008, Lin, Y transformed the original mesh to the frequency domain by using the stream harmonic wave transformation and then embed the watermark, but the shape information will be lost severely in cropping attack [6]. In 2009, Konstantinides embedded the watermarking information into the spherical harmonic coefficient. However this method fully depends on the global match of the mesh, it cannot withstand the cropping attack [7].

On the whole, the frequency domain watermarking algorithm is very complicated and the embedded data is small. In addition, the three-dimensional model is lack of natural parameterization method, so it is difficult to realize the direct frequency domain decomposition for the three-dimensional model. Compared to the frequency domain algorithm, the space domain algorithm has advantage of simple embedding method and large embedding data, so it is valuable in actual practice.

Space domain algorithm: in 1997, Ohbuchi published the first paper on three-dimensional mesh digital watermark [8] and then proposed several watermarking algorithms for the triangle mesh based on the concepts such as mesh replacement, topology replacement and visible mode [9-11]. The most typical and historical algorithms include Triangle Similarity Quadruple (TSQ) algorithm and Tetrahe-dral Volume Ratio (TVR) algorithm. These algorithms

*Address correspondence to this author at the 516 Jun Gong Road, Shanghai, China, 200093, Tel: 13636675266; E-mail: wangwenju666@163.com

1874-4443/15

are very sensitive to the noises and topology change. In 2005, Zafeiriou proposed to embed the watermarking information by changing the vortex coordinate in the spherical coordinate system, but this algorithm cannot resist the affine transformation [12]. In 2008, Salman embedded the watermarking information by using the normal vector of the three-dimensional model, but this algorithm requires the detailed internal organization information on three-dimensional model in extraction of the watermarking information, so this algorithm is only applicable to embedded of the private watermark [13]. In 2009, Wang Yuping and Hu Shimin from Tsinghua University proposed a space domain half vulnerable blind watermarking algorithm based on the integral invariant, which can resist vortex disorder, RST transformation and small noise attack, but this algorithm can easily lead to whole distortion of the original three-dimensional model [14]. In 2009, Qingsongai from Wuhan University of Technology divided the three-dimensional model into multiple Voronoi patches by the three-dimensional model feature points and embedded watermarking information. This algorithm has better anti-tailoring performance, but it will speed much time in dividing Voronoi patch by the selected feature points in advance. So it is difficult to operate and implement [15]. In 2011, Ho L embedded the watermark by using the vertex information of three-dimensional model surface and the progressive mesh compression to protect the three-dimensional detailed model watermark, but the histogram bin shifting technology changes the geometric information of the vortexes [16]. Liu Quan proposed a non-blind watermarking algorithm to construct the spherical coordinate mapping matrix and apply SVD decomposition for constructing a more stable watermarking element to embed the watermark. This algorithm can resist the noises and tailoring, which extremely improves the robustness of the space domain watermarking algorithm, but its calculation is slow due to time complexity $O(N^3)$ of the SVD decomposition [17].

The above space domain watermarking algorithms are intuitive and can embed massive information, but it is difficult to realize the blind watermarking and the robustness is worse. So these algorithms are restricted in actual applications. In addition, most current three-dimensional mesh digital watermark algorithms use pseudorandom sequence [3, 4, 12, 15, 17] or Arnold transformation to realize the scrambling encryption of the watermarking images [14] as the watermarking information. The pseudorandom sequence has a low linear complexity and the Arnold transformation encryption is susceptible to the exhaustive attack. So the above algorithms can be easily decrypted, imitated, which cannot accurately perform the anti-counterfeiting authentication.

Therefore, this paper proposes a holographic digital watermark algorithm based on QR decomposition for three-dimensional mesh model, which is difficult decryption and imitation. This algorithm can resist translation, rotation, scaling, vertex reordering, noise and cropping attack, which has high robustness and high practicable application value.

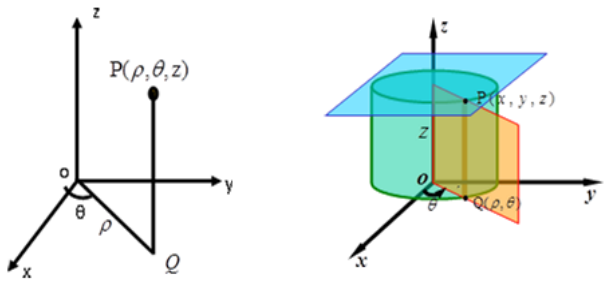

Fig. (1). Cylindrical coordinate system.

The section 2 of this paper gives some preliminary knowledge. The section 3 introduces a holographic digital watermark algorithm based on QR decomposition for three-dimensional mesh model. The section 4 gives the experimental results and analysis. Finally the conclusions are concluded.

2. PRELIMINARY KNOWLEDGE

2.1. Cylindrical Coordinate

Assume that P is any point in the space and is projected as Q on oxy plane. $(\rho,\theta)(\rho \geq 0, 0 \leq \theta < 2\pi)$ indicates the polar coordinate of the point Q on the plane oxy. The position of the point P can be represented with the orderly array (ρ,θ,z), where $\rho \geq 0, 0 \leq \theta < 2\pi, -\infty \leq z \leq +\infty$. The coordinate system with the above mapping is called as the cylindrical coordinate system, shown as the Fig. (**1**). The rectangular coordinate (x,y,z) and polar coordinate (ρ,θ,z) of the space point P can be transformed with the equation (1) and (2).

$$\begin{cases} \rho^2 = x^2 + y^2 \\ \theta = arctg\dfrac{y}{x}(x \neq 0), 0 \leq \theta < 2\pi \\ z = z \end{cases} \quad (1)$$

$$\begin{cases} x = \rho\cos\theta \\ y = \rho\sin\theta \\ z = z \end{cases} \quad (2)$$

If ρ is constant in the cylindrical coordinate, the equation expresses a cylindrical surface. If θ is constant, the equation expresses a half plane. If z is constant, the equation expresses a plane.

2.2. QR Decomposition

As the intermediate computing step in SVD, the time complexity of matrix QR decomposition is $O(N^2)$ [18]. QR decomposition requires less time in computing.

The matrix QR decomposition method includes *Gram – Schmidt Householder* and *Givens* method. The accumulative rounding error of *Gram – Schmidt* algorithm is bigger in computing. When the order of the matrix is bigger, *Givens* method will generate heavy computing workload. So *Householder* method is frequently used in QR decomposition.

Assume the matrix $A \in R^{m \times n}$ and $m \geq n$, QR decomposition of the matrix A can be expressed as the equation (3).

$$A = Q \cdot R \tag{3}$$

$Q = H_1 H_2 \cdots\cdots H_{n-1}$, H_i is obtained *via Householder* transformation of ith column vector in A. Q is a $m \times m$ matrix with the standard orthogonal vector. $R = H_{n-1} \cdots\cdots H_2 H_1 A$, where R is $m \times n$ upper triangle matrix.

Assume that A and Q are expressed as $A = \left[a_1, a_2, \cdots\cdots a_n\right]$ and $Q = \left[q_1, q_2, \cdots\cdots q_m\right]$, $a_i (\mathrm{i} = 1,2,\cdots\cdots \mathrm{n})$ and $q_j (\mathrm{j} = 1,2,\cdots\cdots \mathrm{m})$ are the column vector of the matrix A and Q and include m element, R is expressed as the Eq. (4):

$$\begin{aligned} R &= Q^T \cdot Q \cdot R = Q^T \cdot A \\ &= \left[q_1, q_2, \cdots\cdots q_m\right]^T \cdot \left[a_1, a_2, \cdots\cdots a_n\right] \\ &= \begin{bmatrix} r_{11} & r_{12} & \cdots\cdots & r_{1n} \\ 0 & r_{22} & \cdots\cdots & r_{2n} \\ \vdots & \vdots & \ddots & \vdots \\ 0 & 0 & 0 & r_{mn} \end{bmatrix} \end{aligned} \tag{4}$$

After QR decomposition, the matrix R has an important property. If the columns of the matrix A are associated, the absolute values of the elements in the first row of the matrix R may be bigger than the corresponding elements in other rows. The bigger values permit bigger change range, so the elements of the first row of the matrix R are suitable for embedded of the watermarking information.

2.3. Digital Holographic Information

Now the holographic watermarking theory is only applied into 2D images and is not explored on the three-dimensional images, but it encrypts information by using the double-random phase and has segmentation characteristic (namely fragments can also reflect the whole). With the above features, the watermarking technology based on the optical holographic theory provides a new means to solve the problems such as easy decryption, no accurate anti-counterfeiting authentication, susceptibility to the cropping attack and easy loss of original three-dimensional mesh information.

The digital holographic technology used in this paper refers to the method used by Nobukatsu Takai and belongs to the Fourier transformation holograph [19].

The watermarking image is defined as $g_{mark}(x, y)$. After the watermarking images are modulated by a random phase template, the modulated images can be expressed as:

$$g_0(x, y) = g_{mark}(x, y) \exp[i\phi(x, y)] \tag{5}$$

2D phase $\phi(x, y)$ is determined by the Gauss random number. The modulated watermarking image is processed with the Fourier transformation and interferes with the reference light. The strength distribution field generated by coherence is the Fourier transformation holographic image expected in this paper.

The Fourier transformation of the watermarking images is expressed as follows:

$$G_{mark}(\xi, \eta) = \iint g_0(x, y) \exp[-2\pi(\xi x + \eta y)] dx dy \tag{6}$$

The reference light is defined as:

$$R(\xi, \eta) = R_0 \exp[2\pi i(a\xi + b\eta)] \tag{7}$$

The watermarking images and light field distribution interfere with the reference light are expressed as follows:

$$\begin{aligned} H_1(\xi, \eta) &= \left|G_{mark}(\xi, \eta) + R(\xi, \eta)\right|^2 \\ &= \left|G_{mark}(\xi, \eta)\right|^2 + \left|R(\xi, \eta)\right|^2 \\ &+ G_{mark}{}^*(\xi, \eta) R(\xi, \eta) + G_{mark}(\xi, \eta) R^*(\xi, \eta) \end{aligned} \tag{8}$$

In equation (8), the element 1 and 2 indicate the halo light and center bright point of the Fourier transformation holographic image, which affect reoccurrence of the watermark and has to be removed to get the equation (9).

$$\begin{aligned} H(\xi, \eta) &= G_{mark}{}^*(\xi, \eta) R(\xi, \eta) \\ &+ G_{mark}(\xi, \eta) R^*(\xi, \eta) \end{aligned} \tag{9}$$

Equation (9) expresses the digital holograph to use, which records the amplitude and phase of the physical light wave and is the watermarking signals embedded into the home images.

The light field strength distribution can be obtained by the mathematic expression to describe the reconstructed light multiplied with the holographic images after Fourier transformation. The reconstructed light can be defined as follows:

$S(\xi, \eta) = \left|S(\xi, \eta)\right| \exp[i\phi_s(\xi, \eta)]$. For the simplest case, $\left|S(\xi, \eta)\right| = 1$ and $\phi_s(\xi, \eta) = 0$. The reconstructed images

obtained via the inverse Fourier transformation are expressed as follows:

$$g_R(x,y) = \iint H(\xi,\eta)\exp[2\pi i(\xi x + \eta y)]d\xi d\eta \quad (10)$$

The equation (9), (6) and (7) are substituted into (10) and obtain the reconstructed light field:

$$g_R = g_0^*[(x-a),(y-b)] + g_0[-(x+a),-(y+b)] \quad (11)$$

The equation (11) indicates that the original images and conjugated images redisplay on the same plane. (a,b) and $(-a,-b)$ are their center. The position of the redisplayed images can be controlled by a and b.

3. HOLOGRAPHIC DIGITAL BLIND WATERMARK ALGORITHM OF MESH MODEL

3.1. Embedding Watermark

The specific watermark is embedded as follows:

(1) Generation of optical holographic encrypted watermarking information:

To realize difficult decryption of the watermarking information embedded into three-dimensional model, this paper uses binary image $g_{mark}(x,y)$ ($s \times s$ indicates the size) as the watermarking images, which is processed by the algorithm described in 2.3 and generated the optical holographic encrypted watermarking information $H(\xi,\eta)$. $H(\xi,\eta)$ includes massive double-precision data, so it is difficult to embed this watermark into the three-dimensional mesh model. Generally most watermarking information is binary sequences, referring to the equation (12).

$$w = \{w_i \,|\, w_i \in \{0,1\}\}, 0 \le i \le length - 1 \quad (12)$$

length is the bits of the watermarking information, so $H(\xi,\eta)$ should be transformed to the gray image $H(\mathrm{x},\mathrm{y})$. Each pixel includes 8 bit data in this gray image. The binary sequence information embedded for the three-dimensional model watermarking is the optical holographic encrypted binary sequence information W_{H_i} ($i = 1,2,\cdots length, length = s \times s \times 8$) generated by $H(\mathrm{x},\mathrm{y})$. The optical holographic encrypted watermarking information is generated as the Fig. (**2**).

(2) Pre-process three-dimensional mesh model

Any three-dimensional model is composed of the vertex set V and connections among vertices [6]. For any three-dimensional mesh model O, the number of vertex is n and the vertex set is $V\{\mathrm{v}_i, \mathrm{i} = 1,2,\cdots\cdots \mathrm{n}\}$. In the Cartesian coordinate system, the coordinate of the vertex v_i is $v_i(\mathrm{x}_i,\mathrm{y}_i,\mathrm{z}_i)$.

① Calculation for the center point coordinate

$$v_c(\mathrm{x}_c,\mathrm{y}_c,\mathrm{z}_c) = \frac{1}{n}\sum_{i=1}^{n} v_i(\mathrm{x}_i,\mathrm{y}_i,\mathrm{z}_i) \quad (13)$$

v_i is the ith vertex of three-dimensional model in the equation (13).

② The center is moved to the origin of coordinate:

$$\begin{cases} x_i' = x_i - x_c \\ y_i' = y_i - y_c \\ z_i' = z_i - z_c \end{cases} \quad (14)$$

③ Principal component analysis

To make the three-dimensional mesh model constant to the rotation attack, this paper automatically adjust the model to the unique posture for calibration and preprocessing by using PCA [20]. The covariance matrix C_v of three-dimensional model vertex is shown as the equation (15).

$$C_v = \begin{bmatrix} \sum_{i=1}^{n}(\mathrm{x}_i')^2 & \sum_{i=1}^{n}\mathrm{x}_i' y_i' & \sum_{i=1}^{n}\mathrm{x}_i' z_i' \\ \sum_{i=1}^{n}\mathrm{x}_i' y_i' & \sum_{i=1}^{n}(\mathrm{y}_i')^2 & \sum_{i=1}^{n} y_i' z_i' \\ \sum_{i=1}^{n}\mathrm{x}_i' z_i' & \sum_{i=1}^{n} y_i' z_i' & \sum_{i=1}^{n}(\mathrm{z}_i')^2 \end{bmatrix} \quad (15)$$

Three matrix eigenvalues of C_v is calculated and sorted by descending order $\lambda_{\max}, \lambda_{\mathrm{mid}}, \lambda_{\min}$. The corresponding eigenvector is $\eta_{\max}, \eta_{\mathrm{mid}}, \eta_{\min}$. The maximum eigenvalue $\lambda_{\max}$ and corresponding eigenvector $\eta_{\max}$ act as the principal component p_c of the three-dimensional model. The angle α between $\eta_{\min}$ and y axis is computed. $\eta_{\min}$ is rotated by α to align with y axis, which identifies the rotary matrix T_1. The angle β between η_{mid} and x axis is calculated. η_{mid} is rotated by β to align with x axis, which identifies the rotary matrix T_2.

After the three-dimensional model is analyzed with PCA method, shown as the equation (16), the vertex coordinate of three-dimensional model can be expressed as $v_i''(\mathrm{x}_i'',\mathrm{y}_i'',\mathrm{z}_i'')$. At this time, the principal component direction p_c of three-dimensional model is overlapped with z axis, so the three-dimensional model can be adjusted to the unique posture and orientation.

$$v_i'' = v_i' \times T_1 \times T_2 \quad (16)$$

④ The vertex $v_i''(\mathrm{x}_i'',\mathrm{y}_i'',\mathrm{z}_i'')$ in the Cartesian coordinate system is transformed into the coordinate

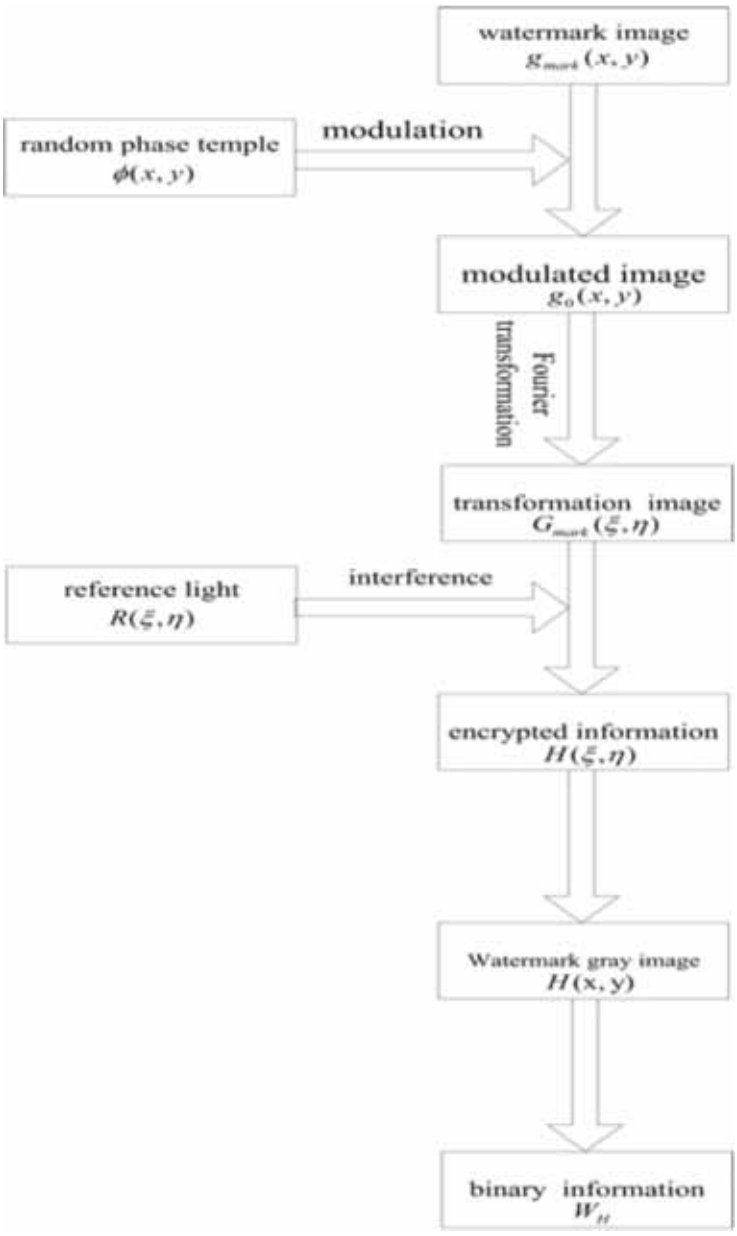

Fig. (2). Generation of watermarking information.

$v_i''(\rho_i'',\theta_i'',z_i'')$ $0 \le \theta_i'' < 2\pi$ in the cylindrical coordinate system by equation (1).

(3) Construction of geometric feature matrix

The vertex $v_i''(\rho_i'',\theta_i'',z_i'')$ is sorted by Z in descending order. z values of partial vertices are same, they will be classified into one class as one sub-set V_{sub} of the vertex set V_i. The number of sub-nets divided from the vertex set V_i by z value is expressed as n_z, $n_z \in [1,n]$.

The vertex set V_i will be sorted by θ in the ascending order. If partial vertices have same θ values, they will be classified into one class as one subset $V_{\theta j}$ of the vertex set V_i. The number of sub-nets divided from the vortex set V_i by θ value is expressed as $n_{\bar{\theta}}$, $n_{\bar{\theta}} \in [1,n]$. The vertices are sorted by z value in descending order in each subset $V_{\theta j}$. If partial vertices have same z value, they will be classified into one class as one subset $V_{\theta jk}$ of $V_{\theta j}$. The distance from vertex to the model center in this subset is $d_{v_k} = \sqrt{\rho_{v_k}^{\ 2} + z_{v_k}^{\ 2}}, v_k \in V_{\theta jk}$. All vertices in $V_{\theta jk}$ will be sorted in the ascending order. The number num_{jk} of vertices in subset $V_{\theta jk}$ is computed and compared to get the vertex number of the maximum subset namely max(num_{jk}) in $V_{\theta j}$.

The three-dimensional mesh model in cylindrical coordinate system can be expressed with the matrix $D[n_z, n_\theta]$, $n_\theta = \sum_{j=1}^{n_{\bar{\theta}}} \max(num_{jk})$. D[i, j] indicates the distance from the vertex v_{ij} to the model center, which identified by θ value and in the ith subset divided by z value $d_{i,j} = \sqrt{\rho_{ij}^{\ 2} + z_{ij}^{\ 2}}$ where ρ_{ij} indicates the polar coordinate radius of this vertex on the plane oxy. z_{ij} indicates the z value of this vertex in the cylindrical coordinate. If no vertex is available in D[i, j], $d_{i,j} = 0$. The ith row has the same z value and the jth column has same θ values in the matrix $D[n_z, n_\theta]$.

The matrix D can store d value of $n_z \times n_\theta$ vertices, which is far bigger than the vertex number of the three-dimensional mesh model, so D includes massive 0 values and is a sparse matrix. The three-dimensional model surfaces are different, so distribution of 0 value is so different in the matrix D that it is difficult to find the rule for further processing. Non-zero d_{ij} values in D are obtained by the row sequence to construct a non-negative real number sequence $\overline{d} = (d_1, d_2, \cdots\cdots d_n)$ with the length n.

Assume $L = \lfloor \sqrt{n} \rfloor$, the following vector is defined:

$$D_K' = (d_{(K-1)L+1}, d_{(K-1)L+2}, \cdots\cdots d_{KL})^T \tag{17}$$

where $1 \le K \le L$.

The model's geometric feature matrix is obtained, referring to the equation (18)

$$D' = (D_1', D_2', \cdots\cdots D_L') = \begin{bmatrix} d_1' & d_{L+1}' \cdots d_{(L-1)L+1}' \\ d_2' & d_{L+2}' \cdots d_{(L-1)L+2}' \\ \vdots & \ddots \ \vdots \\ d_L' & d_{2L}' \cdots\cdots d_{L\times L}' \end{bmatrix} \tag{18}$$

(4) QR decomposition and watermarking

① Normalization of the elements in the geometric feature matrix D' indicates to normalize the distances from all vertices to the model center namely $d_{ij}' \in [0,1]$ by using the equation (19).

$$\begin{cases} d_{\min}' = \min\left\{ d_{ij}' \middle| d_{ij}' \in D' \right\} \\ d_{\max}' = \max\left\{ d_{ij}' \middle| d_{ij}' \in D' \right\} \\ d_{ij}'' = \dfrac{d_{ij}' - d_{\min}'}{d_{\max}' - d_{\min}'} \end{cases} \tag{19}$$

In the equation (19), $d_{\min}$ indicates the minimal distance from the vertices to the model center v_c in the vertex set V_i. $d_{\max}$ indicates the maximal distance from the vertex to the model center v_c in the vertex set V_i. d_{ij}' indicates the distance from the vortexes to the model center v_c. d_{ij}'' indicates the normalized result values.

② Block division of matrix

The geometric feature matrix D' is divided into $N_m = \left\lfloor \dfrac{s \times s \times 8}{m} \right\rfloor$ non-overlapping matrix blocks with the size $s \times s$. $s \times s$ is the size of binary watermarking image $g_{mark}(x, y)$ and m is the row number and column number of QR decomposition matrix.

③ QR decomposition

QR decomposition is performed for each selected matrix with the size $m \times m$ according to the equation (3).

④ Embedding watermark

The watermarking information W_{H_i} is embedded by changing the element $r_{11}, r_{12} \cdots\cdots r_{1m}$ in the first row of the matrix R via the following process:

$\min = \min(r_{1j})\ j = 1,2,\cdots m, \max = \max(r_{1j})\ j = 1,2,\cdots m$, Δ refers to the equation (20).

$$\Delta = \frac{\max - \min}{m} \tag{20}$$

With min as the start point, as the quantification interval Δ is used to quantify $r_{1j}(j = 1,2\cdots m)$, referring to the equation (21) and (22).

$$M = round\left[(r_{1j} - \min) \Big/ \Delta \right] \tag{21}$$

$$r_{1j}^{\ *} = \min + \begin{cases} \left.\begin{matrix} M_j \times \Delta, M_j\ is even \\ (M_j - 1) \times \Delta, M_j\ is odd \end{matrix}\right\} w_{H_i} = 0 \\ \left.\begin{matrix} (M_j + 1) \times \Delta, M_j\ is even \\ M_j \times \Delta, M_j\ is odd \end{matrix}\right\} w_{H_i} = 1 \end{cases} \tag{22}$$

⑤ Inverse *QR* decomposition

r_{1j} is replaced with the quantified $r_{1j}^{\ *}$ and performed inverse *QR* decomposition by using the equation (23) to get the matrix with the watermark.

$$D^* = Q \times R^* \tag{23}$$

⑥ Repeat

Repeatedly execute ③-⑤ till all watermarking information is embedded into the geometric feature matrix of the three-dimensional model.

⑦ Inverse normalization of elements in the geometric feature matrix D^* is executed, referring to the equation (24).

$$d^{w}_{ij} = d^{*}_{ij}(d'_{\max} - d'_{\min}) + d'_{\min}, d^{*}_{ij} \in D^{*} \tag{24}$$

⑧ The cylindrical coordinate of the vertices is transformed to the Cartesian coordinate by equation (25).

$$\begin{cases} \rho^{w}_{ij} = \sqrt{(d^{w}_{ij})^2 - (z^{w}_{ij})^2} \\ x^{w}_{ij} = \rho^{w}_{ij}\cos\theta + x_c \\ y^{w}_{ij} = \rho^{w}_{ij}\sin\theta + y_c \\ z^{w}_{ij} = z^{w}_{ij} + z_c \end{cases} \tag{25}$$

⑨ The three-dimensional model is adjusted to the original posture and orientation.

T_2' indicates the rotation matrix with x axis rotating $(-\beta)$. T_1' indicates the rotation matrix with y axis rotating $(-\alpha)$ in the equation (26).

$$v_i^{w'} = v_i^{w} \times T_2' \times T_1' \tag{26}$$

After the above steps, the watermarking data can be embedded into the three-dimensional model with the watermark.

3.2. Extraction of Watermarking Information

The original watermarking image and original three-dimensional model are not required in watermark extraction algorithm. So this algorithm is blind. The specific watermark extraction process is described as follows:

(1) Pre-processing of mesh model with watermark

The three-dimensional model which may include watermark, is pre-processed by using the method above mentioned in this paper. The geometric feature matrix is constructed in the cylindrical coordinate system and is normalized to get the matrix D'.

(2) Block processing of matrix

The geometric feature matrix D' is divided into $m \times m$ non-overlapping matrix blocks.

(3) QR decomposition

QR decomposition is performed for each geometric feature matrix with watermark according to the equation (3) to get the matrix R^*.

(4) Extract watermark

Δ is computed again according to $r^{*}_{1j}(\mathrm{j}=1,2\cdots m)$, $\min, \max, .$

Extract the watermark $w^{*}_{H_i}$ from the element $r^{*}_{1j}(\mathrm{j}=1,2\cdots m)$ in the first row of the matrix R^* by using the equation (27).

$$w^{*}_{H_i} = \begin{cases} 0 \; if \; round(\left(\mathrm{r}_{1j}{}^{*} - \min\right) \Big/ \Delta) \text{ is even} \\ 1 \; if \; round(\left(\mathrm{r}_{1j}{}^{*} - \min\right) \Big/ \Delta) \text{ is odd} \end{cases} \tag{27}$$

(5) Repeat

The step (2)-(4) is repeatedly executed till all matrix blocks with embedded watermark are treated. The extracted watermark sequence $w^{*}_{H_i}$ is grouped with 8 bits as one group. The binary data of each group is transformed to the decimal data values. The final data is stored as the gray image $H^{*}(\mathrm{x},\mathrm{y})$.

(6) Optical holographic decryption

Fourier transformation for the gray images is performed according to the equation (10) and filterred with 2-order Butterworth high-pass filter to get binary watermarking image $g^{*}_{mark}(x,y)$.

4. EXPERIMENTAL RESULTS AND ANALYSIS

To check the performance of the watermarking algorithm proposed, this paper realizes a three-dimensional model watermarking prototype system by using Matlab2013 as the experimental platform. The three-dimensional model Stanford Bunny, Horse and Dragon provided at http://www.cc.gatech.edu/projects/large_models/ is used as the home image. Stanford Bunny model includes 35947 vertices and 69451 triangle faces. Horse model includes 48485 vertices and 96966 triangle faces. Dragon model includes 50000 vertices and 100000 triangle faces. Binary image of size 32×32 is selected as the watermarking image. The size of QR decomposition matrix is 4×4, namely $s = 32$, $m = 4$. The used model and binary watermarking image refer to the Fig. (**3**).

The watermarking mesh model experiences some processing, transformation or attacks, the extracted watermark may not be fully same with the embedded watermark. To assess the robustness of this watermarking algorithm, we compute the related coefficients between extracting the watermark sequence and embedded the watermark sequence [3], referring to the equation (28)

$$corr = \frac{\sum_{i=1}^{length} (\mathrm{w}_i - \bar{\mathrm{w}})(\mathrm{w}'_i - \bar{\mathrm{w}}')}{\sqrt{\sum_{i=1}^{length} (\mathrm{w}_i - \bar{\mathrm{w}}) \sum_{i=1}^{length} (\mathrm{w}'_i - \bar{\mathrm{w}}')}} \tag{28}$$

Fig. (3). Original models and watermarking image.

Table 1. Robustness for affine attack and reordering attack.

Model	corr of Rotation Attack	corr of Translation Attack	Corr Of Scaling Attack	corr of Reordering Attack
Bunny	1	1	1	1
Horse	1	1	1	1
Dragon	1	1	1	1

Model rotates by angle of 35 degree Model scales by 0.3

Holographic encrypted image Recovered watermark image

Fig. (4). Affine transformation attack.

w_i is the embedded watermark W_{H_i}. w_i' is the extracted watermark $w_{H_i}^*$ to determine. $\overline{\mathrm{w}}$ is the mean of w_i and $\overline{\mathrm{w}}'$ is the mean of $\overline{\mathrm{w}}$.

$corr \in [0,1]$. Bigger $corr$ indicates higher similarity of the watermark and stronger robustness of the watermark in this algorithm.

To detect the attack effect of the algorithm, this paper tests multiple attacks. The results and analysis are described as follows:

(1) Vertex reordering attack

Two vertices randomly selected are exchanged their sequence and repeated $10 \times n$ times. n indicates the number of the vertices in the model. The experimental results (shown as the Table **1**) indicates that the watermarking information can be completely extracted after reoredering attack because the distances from the vertices to the model center are sorted by z and θ value in construction of the model's geometric feature matrix. The same processing is required in watermark extraction to ensure that the geometric feature matrix of the model keep constant for the vertex reordering attack. So the vertex reordering attack will not affect watermark extraction.

(2) Affine transformation attack

The affine transformation attacks include rotation, translation and scaling. The three-dimensional model Dragon with watermark rotates by angle of 35 degree around z axis and scales by 0.3, the effect is shown as the Fig. (**4**). The experimental results of translation, rotation and scaling attack are shown as the Table **1**. For the mesh the watermark extraction is done after the origin of coordinate moves the model center, so the translation attack will

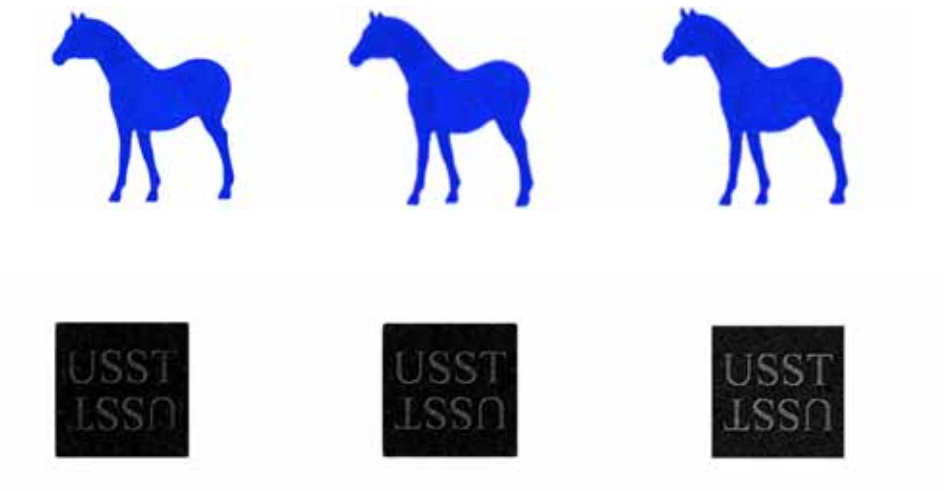

Fig. (5). Noise attack effect number, sequence and topology as the original model.

Table 2. Model robustness for noise attack.

Model	Noise strength	corr
Bunny	0.1%	0.8634
	0.2%	0.8478
	0.3%	0.7356
Horse	0.1%	0.8718
	0.2%	0.8536
	0.3%	0.7489
Dragon	0.1%	0.8836
	0.2%	0.8615
	0.3%	0.7658

not affect the watermark extraction. The PCA method is used for automated alignment to make the watermarking three-dimensional model keep same orientation and posture before and after attack, so the rotation operation will not affect the watermark extraction. After the elements of the geometric feature matrix are normalized, the watermark is embedded and extracted. So the scaling attack will not affect watermark extraction.

(3) Noise attack

A random noise vector is added for each vertex in three-dimensional model and the length of this vector is 0.1%, 0.2% and 0.3% of the mean distance from the vertices to the model center. The experimental effect is shown as the Fig. (**5**). The experimental results are shown as the Table **2**. When the noise strength reaches 0.3%, the watermark still can be extracted because the watermarking information is embedded into the elements of the first row in R matrix obtained after QR decomposition. These elements in this row are biggest in the whole R matrix. Their small change will not lead to information extraction failure. It indicates that QR decomposition is very stable.

(4) Cropping attack

For cropping attack, the vertex number and topology of the three-dimensional model will change. The re-sampling method [4] will be used to recover the vertex

0.1% noise 0.2% noise 0.3% noise

① Cropping attack

After the Stanford Bunny model with the watermarking information is cropped, the effect is shown as the Fig. (**6**). The experimental effect of the cropping attack is shown as the Table **3**.

From the cropping attack results in the Fig. (**6**), even the cropping rate of the Stanford Bunny model reaches 86%, the extracted watermarking image can be clearly seen

Table 3. Model robustness for cropping attack.

Model	Noise Strenth	corr
Bunny	68%	0.8495
	86%	0.6115
Horse	68%	0.8595
	86%	0.6245
Dragon	68%	0.8652
	86%	0.6354

86% cropping rate 68% cropping rate

Fig. (6). Cropping attack effect.

because the embedded watermarking information is processed with the optical holographic encrypted technology which can resist the cropping well.

CONCLUSION

At present, the spare domain mesh blind watermarking algorithms have some problems such as difficult implementation, worse robustness and easy decryption, so this paper proposes a three-dimensional mesh model optical holographic blind digital watermark algorithm based on QR decomposition. This algorithm pre-processes the three-dimensional model, embeds the watermarking information generated by the optical holographic encrypted technology into the normalized and blocked model's geometric feature matrix with QR decomposition. With Inverse QR decomposition and inverse normalization performed, the watermark finally is embedded into three-dimensional mesh model. The experimental results indicate that this algorithm can resist translation, scaling, vertex reordering, noise and cropping attack, having the higher robustness and important application value. Now this algorithm requires much computing time, so we will improve this algorithm by using the GPU-based parallel computing method for the QR decomposition of the model's geometric feature matrix to further speed up this algorithm.

CONFLICT OF INTEREST

The authors confirm that this article content has no conflict of interest.

ACKNOWLEDGEMENTS

This work was supported in part by a grant from the Starting Project of Doctor of University of Shanghai for Science and Technology (No. 1D-13-309-005), Funding Scheme for Training Young teachers in Shanghai Colleges in 2013 (No. slg14039), Innovation Program of Shanghai Municipal Education Commission (No. 13ZZ111), the bidding project of Shanghai research institute of publishing and media (No. SAYB1409) funded by the National Higher Vocational and Technical Colleges construction project of the Shanghai Publishing and Printing College.

REFERENCES

[1] B.T. Andrade, C.M. Mendes, J.O. Santos Jr., O.R.P. Bellon, and L. Silva, "Three-Dimensional Preserving xviii Century Barroque Masterpiece: Challenges and Results on the Digital Preservation of Aleijadinho's Sculpture of the Prophet Joel", *J. Cultural Heritage*, vol. 13, pp. 210-214, Jun. 2012.

[2] K. Wang, G. Lavoué, F. Denis, and A. Baskurt, "A Comprehensive Survey on Three-Dimensional Mesh Watermarking", *IEEE Trans. Multimedia*, vol. 10, pp. 1513-1527, Dec. 2008.

[3] E. Praun, H. Hoppe, and A. Finkelstein, "Robust Mesh Watermarking", In: *Computer Graphics Proceedings, Annual Conference Series*, ACM SIGGRAPH, 1999, pp. 49-56.

[4] R. Ohbuchi, S. Takahashi, T. Miyazawa and A. Mukaiyama, "Watermarking Three-Dimensional Polygonal Meshes in the Mesh Spectral Domain", In: *Proceedings of Graphics Inter-face*, pp. 9-17, 2001.

[5] K. Wang, G. Lavoue, F. Denis, and A. Baskurt "Hierarchical Watermarking of Semiregular Meshes Based on Wavelet Transform", *IEEE Trans. Inf. Forensics Security*, vol. 3, pp. 620-634, Dec.2008.

[6] Y.P. Liu, "A robust spectral approach for blind watermarking of manifold surfaces", In: *Proceedings of the 10th ACM Workshop on Multimedia and Securit*, 2008, pp. 43-52.

[7] J.M. Konstantinides, A. Mademlis, P. Daras, P.A. Mitkas, and M.G. Strintzis, "Blind ROBUST 3-D mesh watermarking based on oblate spheroidal harmonics", *IEEE Trans. Multimedia*, vol. 11, pp. 23-38, Jan. 2009.

[8] R. Ohbuchi, H. Masuda, and N. Aono, "Watermarking Three-Dimensional Polygonal Models", In: P*roceedings of ACM Multimedia 97*, 1997, pp. 261-272.

[9] R. Ohbuchi, H. Masuda, and N. Aono, "Embedding Data in Three-Dimensional Models", In*: Proceedings of the 1997 4th International Workshop on Interactive Distributed Multimedia Systems and Telecommunication Services*, 1997, pp. 1-10.

[10] R. Ohbuchi, H. Masuda, and N. Aono, "Watermarking Three-Dimensional Polygonal Models Through Geometric and Topological Modification", *IEEE J. Sel. Areas Commun.*, vol. 16, pp. 551-560, May 1998.

[11] R. Ohbuchi, H. Masuda, and N. Aono, "Watermarking Multiple Object Types in Three-Dimensional Models", In: *Proceedings of the Workshop on Multimedia & Security at ACM Multimedia'98*, 1998, pp. 83-91.

[12] S. Zafeiriou, A. Tefas, and I. Pitas, "Blind Robust Watermarking Schemes for Copyright Protection of Three-Dimensional Mesh Objects", *IEEE Trans. Vis. Comput. Graph.*, vol. 11, pp. 596-607, Sep. 2005.

[13] M. Salman, Z. Ahmad, S. Worrall, and A.M. Kondoz, "Robust Watermarking of 3-D Polygonal Models", In: *3rd International Symposium on Communications, Control and Signal Processing*, 2008, pp. 340-343.

[14] Y. Wang, and S. Hu, "A New Watermarking Method for Three-Dimensional Models Based on Integral Invariants", *IEEE Trans. Vis. Comput. Graph.*, vol. 15, pp. 285-294, Mar. 2009.

[15] Q.S. Ai, Q. Liu, Z.D. Zhou, L. Yang, and S. Q. Xie, "A new digital watermark scheme for three-dimensional triangular mesh models", *Signal Proces.*, vol. 89, pp. 2159-2170, Nov. 2009.

[16] H. Lee, C. Dikici, G. Lavoue, and F. Dupont, "Joint reversible watermarking and progressive compression of three-dimensional meshes", *Visual Comput.*, vol. 27, pp. 6-8, June 2011.

[17] Q. Liu and X. Zhang, "SVD Based Digital Watermark Algorithm for Three-Dimensional Models", In: *International Conference on Signal Processing Proceedings*, 2007, pp. 1-6.

[18] Q. Su, Y. Niu, G. Wang, S. Jia, and J. Yue, "Color image blind watermarking scheme based on qr decomposition", *Signal Proces.*, vol. 94, pp. 219-235, January 2014.

[19] N. Takai, and Y. Mifune, "Digital watermark by a holographic technique", *Appl. Opt.*, vol. 41, pp. 865-873, Feb 2002.

[20] A. Kalivas, A. Tefas, and I. Pitas, *Watermarking of Three-Dimensional Models Using Principal Component Analysis*, 2003, pp. 676-679.

Received: September 16, 2014 Revised: December 23, 2014 Accepted: December 31, 2014